

# Similarity Renormalization Group for Nucleon-Nucleon Interactions

S.K. Bogner,\* R.J. Furnstahl,† and R.J. Perry‡

*Department of Physics, The Ohio State University, Columbus, OH 43210*

(Dated: February 9, 2020)

The similarity renormalization group (SRG) is based on unitary transformations that suppress off-diagonal matrix elements, forcing the hamiltonian towards a band-diagonal form. A simple SRG transformation applied to nucleon-nucleon interactions leads to greatly improved convergence properties while preserving observables, and provides a method to consistently evolve many-body potentials and other operators.

PACS numbers: 21.30.-x,05.10.Cc,13.75.Cs

Progress on the nuclear many-body problem has been hindered for decades because nucleon-nucleon (NN) potentials that reproduce elastic scattering phase shifts typically exhibit strong short-range repulsion as well as a strong tensor force. This leads to strongly correlated many-body wave functions and highly nonperturbative few- and many-body systems. But recent work shows how a cutoff on relative momentum can be imposed and evolved to lower values using renormalization group (RG) methods, thus eliminating the troublesome high-momentum modes [1, 2]. The evolved NN potentials are energy-independent and preserve two-nucleon observables for relative momenta up to the cutoff. Such potentials, known generically as  $V_{\text{low } k}$ , are more perturbative and generate much less correlated wave functions [2, 3, 4, 5, 6, 7], vastly simplifying the many-body problem. However, a full RG evolution of essential few-body potentials has not yet been achieved.

An alternative path to decoupling high-momentum from low-momentum physics is the similarity renormalization group (SRG), which is based on unitary transformations that suppress off-diagonal matrix elements, driving the hamiltonian towards a band-diagonal form [8, 9, 10, 11]. The SRG potentials are automatically energy independent and have the feature that high-energy phase shifts (and other high-energy NN observables), while typically highly model dependent, are preserved, unlike the case with  $V_{\text{low } k}$  as usually implemented. Most important, *the same transformations renormalize all operators*, including many-body operators, and the class of transformations can be tailored for effectiveness in particular problems.

Here we make the first exploration of SRG for nucleon-nucleon interactions, using a particularly simple choice of SRG transformation, which nevertheless works exceedingly well. We find the same benefits of  $V_{\text{low } k}$ : more perturbative interactions and lessened correlations, with improved convergence in few- and many-body calcula-

tions. The success of the SRG combined with advances in chiral effective field theory (EFT) [12, 13] opens the door to the consistent construction and RG evolution of many-body potentials and other operators.

The similarity RG approach was developed independently by Glazek and Wilson [8] and by Wegner [9]. We follow Wegner's formulation in terms of a flow equation for the hamiltonian. The initial hamiltonian in the center of mass  $H = T_{\text{rel}} + V$ , where  $T_{\text{rel}}$  is the relative kinetic energy, is transformed by the unitary operator  $U(s)$  according to

$$H_s = U(s) H U^\dagger(s) \equiv T_{\text{rel}} + V_s , \quad (1)$$

where  $s$  is the flow parameter. This also defines the evolved potential  $V_s$ , with  $T_{\text{rel}}$  taken to be independent of  $s$ . Then  $H_s$  evolves according to

$$\frac{dH_s}{ds} = [\eta(s), H_s] , \quad (2)$$

with

$$\eta(s) = \frac{dU(s)}{ds} U^\dagger(s) = -\eta^\dagger(s) . \quad (3)$$

Choosing  $\eta(s)$  specifies the transformation. Here we make perhaps the simplest choice [10],

$$\eta(s) = [T_{\text{rel}}, H_s] , \quad (4)$$

which gives the flow equation,

$$\frac{dH_s}{ds} = [[T_{\text{rel}}, H_s], H_s] . \quad (5)$$

Other choices will be studied elsewhere [14].

For any given partial wave in the space of relative momentum NN states, Eq. (5) means that the potential in momentum space evolves as (with normalization so that  $1 = \frac{2}{\pi} \int_0^\infty |q| q^2 dq \langle q |$  and in units where  $\hbar^2/M = 1$ ),

$$\begin{aligned} \frac{dV_s(k, k')}{ds} = & -(k^2 - k'^2)^2 V_s(k, k') \\ & + \frac{2}{\pi} \int_0^\infty q^2 dq (k^2 + k'^2 - 2q^2) \\ & \times V_s(k, q) V_s(q, k') . \end{aligned} \quad (6)$$

\*Electronic address: bogner@mps.ohio-state.edu

†Electronic address: furnstahl.1@osu.edu

‡Electronic address: perry.6@osu.edu

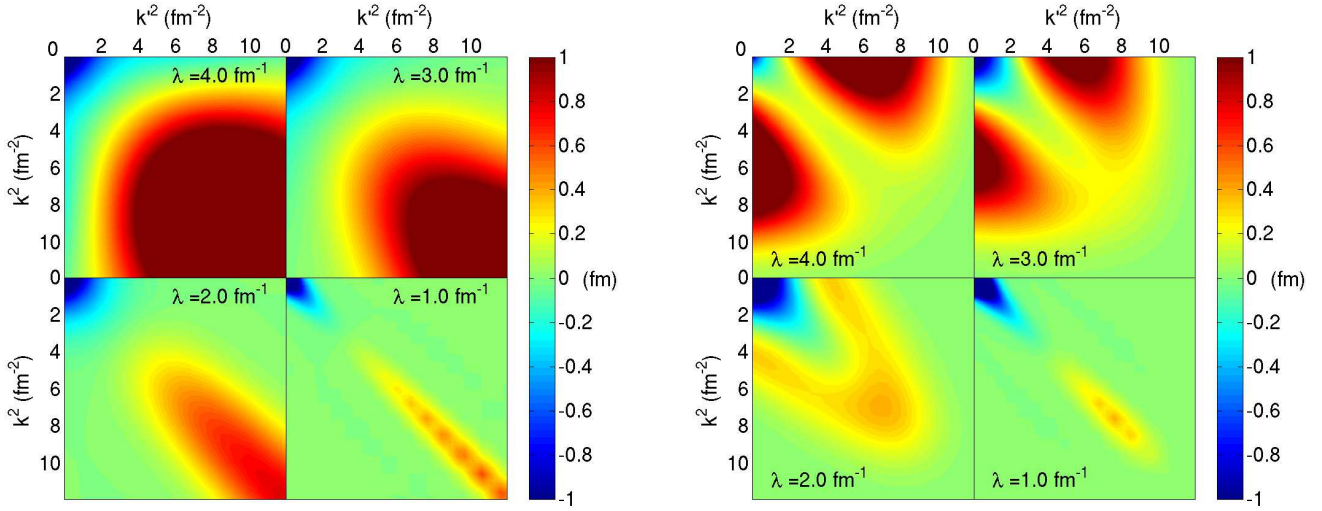


FIG. 1: Contour plots illustrating the evolution of the  $^1S_0$  (left) and  $^3S_1$  (right) potentials with  $\lambda \equiv s^{-1/4}$ . The initial potential on the left is a chiral N<sup>3</sup>LO potential with a 600 MeV cutoff [12] and on the right is an N<sup>3</sup>LO potential with a 550 MeV cutoff on the Lippmann-Schwinger equation and a 600 MeV cutoff on a regularized spectral representation of two-pion exchange [13].

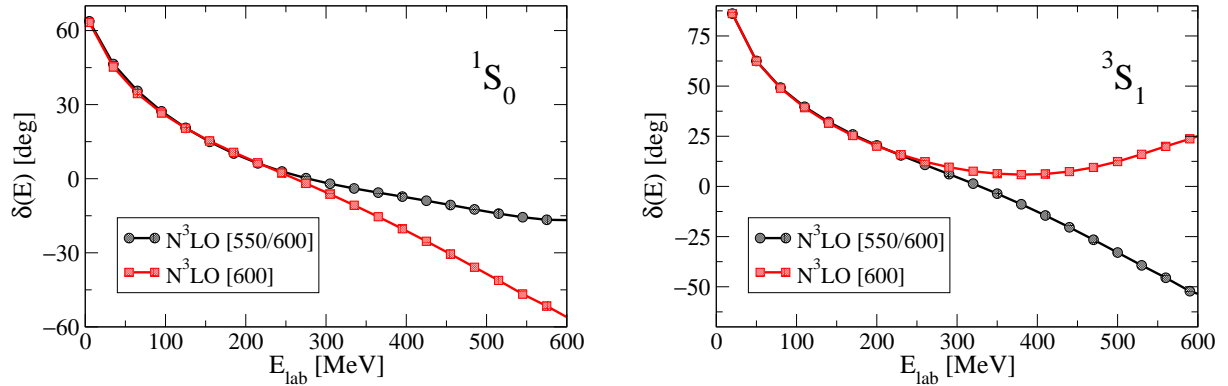


FIG. 2: S-wave phase shifts after evolving in  $\lambda$  starting from the two chiral EFT N<sup>3</sup>LO potentials from Fig. 1. For each initial potential, the phase shifts for different  $\lambda$  agree to within the widths of the lines at all energies shown.

(The additional matrix structure of  $V_s$  in coupled channels such as  $^3S_1$ – $^3D_1$  is implicit.) For matrix elements far from the diagonal, the first term on the right side of Eq. (6) evidently dominates and exponentially suppresses these elements as  $s$  increases. The parameter  $\lambda \equiv s^{-1/4}$  provides a measure of the spread of off-diagonal strength. While further analytic analysis is possible, we instead turn to a numerical demonstration that the flow toward the diagonal is a general result. By discretizing the relative momentum space on a grid of gaussian integration points, we obtain a simple (but nonlinear) system of first-order coupled differential equations, with the boundary condition that  $V_s(k, k')$  at the initial  $s$  (or  $\lambda$ ) is equal to the initial potential.

The evolution of the hamiltonian according to Eq. (6) as  $s$  increases (or  $\lambda$  decreases) is illustrated in Fig. 1, using two initial chiral EFT potentials [12, 13]. On the left is  $^1S_0$  starting from the harder (600 MeV cutoff) potential from Ref. [12], which has significant strength near

the high-momentum diagonal, and on the right is the S-wave part of the  $^3S_1$ – $^3D_1$  coupled channel starting from one of the potentials from Ref. [13], which has more far off-diagonal strength initially and comparatively weaker higher-momentum strength on the diagonal. The initial momentum-space potential differs significantly among interactions that are phase-equivalent up to the NN inelastic threshold, but these examples show characteristic features of the evolution in  $\lambda$ . In particular, we see a systematic suppression of off-diagonal strength, as anticipated, with the width of the diagonal scaling as  $\lambda^2$ .

Since the SRG transformation is unitary, observables are unchanged at *all* energies, up to numerical errors. This is shown by Fig. 2, in which phase shifts for the two chiral EFT potentials are plotted, including the values at high energies where they are not constrained by data (above  $E_{\text{lab}} = 300$  MeV). For a given potential, there is no visible variation with  $\lambda$ . Similarly, the binding energy and asymptotic normalizations for the deuteron are

independent of  $\lambda$  [14].

As  $\lambda$  is lowered, different initial potentials flow to similar forms at low momentum while remaining distinct at higher momentum. The low-momentum parts also become similar to  $V_{\text{low } k}$  potentials. These observations are illustrated in Fig. 3 for two particular slices of the potentials from Fig. 1. They will be explored in much greater detail in Ref. [14].

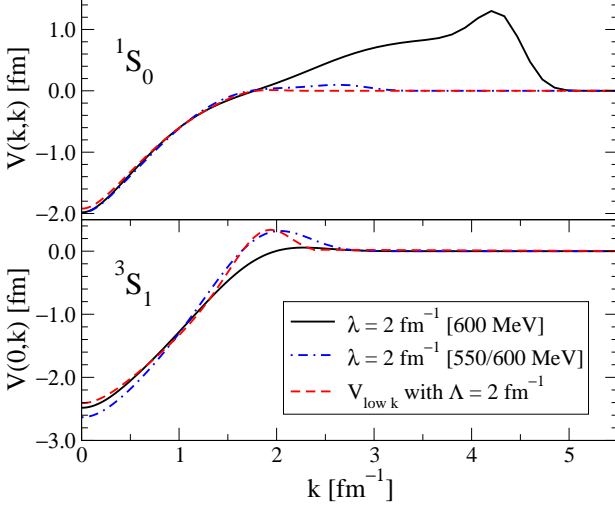


FIG. 3: Matrix elements of the evolved SRG potentials at  $\lambda = 2 \text{ fm}^{-1}$  for  $^1\text{S}_0$  (top, diagonal elements) and  $^3\text{S}_1$  (bottom, off-diagonal elements) for the same initial potentials as in Fig. 1. Also shown is the  $V_{\text{low } k}$  potential with a smooth (exponential) regulator for momentum cutoff  $\Lambda = 2 \text{ fm}^{-1}$ , from the two potentials (600 MeV above and 550/600 MeV below).

We can quantify the perturbativeness of the potential as we evolve to lower  $\lambda$  by using the eigenvalue analysis introduced long ago by Weinberg [15] and recently applied in an analysis of  $V_{\text{low } k}$  potentials [6]. Consider the operator Born series for the  $T$ -matrix at energy  $E$  (for simplicity we assume  $E \leq 0$ ):

$$T(E) = V_s + V_s \frac{1}{E - T_{\text{rel}}} V_s + \dots \quad (7)$$

By finding the eigenvalues and eigenvectors of

$$\frac{1}{E - T_{\text{rel}}} V_s |\Gamma_\nu\rangle = \eta_\nu(E) |\Gamma_\nu\rangle, \quad (8)$$

and then acting with  $T(E)$  on the eigenvectors,

$$T(E) |\Gamma_\nu\rangle = V_s |\Gamma_\nu\rangle (1 + \eta_\nu + \eta_\nu^2 + \dots), \quad (9)$$

it follows that nonperturbative behavior at energy  $E$  is signaled by one or more eigenvalues with  $|\eta_\nu(E)| \geq 1$  [15]. (See Ref. [6] for a more detailed discussion in the context of evolving  $V_{\text{low } k}$  potentials.)

It suffices for our purposes to consider a single energy (e.g.,  $E = 0$ ), and to consider only the negative eigenvalues, which are associated with the short-range repulsion.

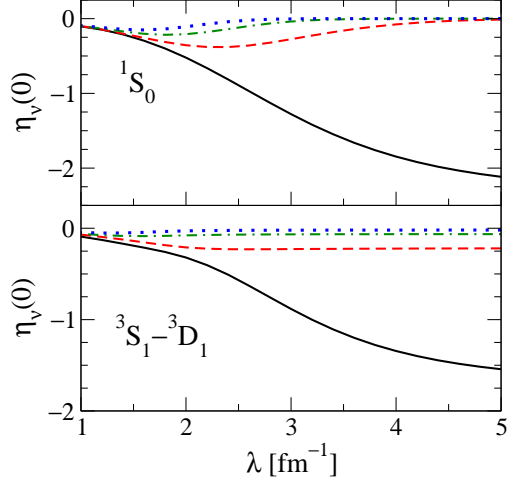


FIG. 4: The largest repulsive Weinberg eigenvalues as a function of  $\lambda$  in the  $^1\text{S}_0$  channel and the  $^3\text{S}_1 - ^3\text{D}_1$  coupled channel for the same initial potentials as in Fig. 1.

Weinberg eigenvalues at zero energy are shown as a function of  $\lambda$  in Fig. 4 for the  $^1\text{S}_0$  channel and the  $^3\text{S}_1 - ^3\text{D}_1$  coupled channel. In both channels, the large negative eigenvalues at large  $\lambda$  reflect the repulsive core of the initial potentials. They rapidly evolve to small values as  $\lambda$  decreases to  $2 \text{ fm}^{-1}$  and below, as also observed with the  $V_{\text{low } k}$  evolution [6]. However, the intermediate increase for the sub-leading eigenvalues in  $^1\text{S}_0$  is a new feature of the SRG that merits further study [14].

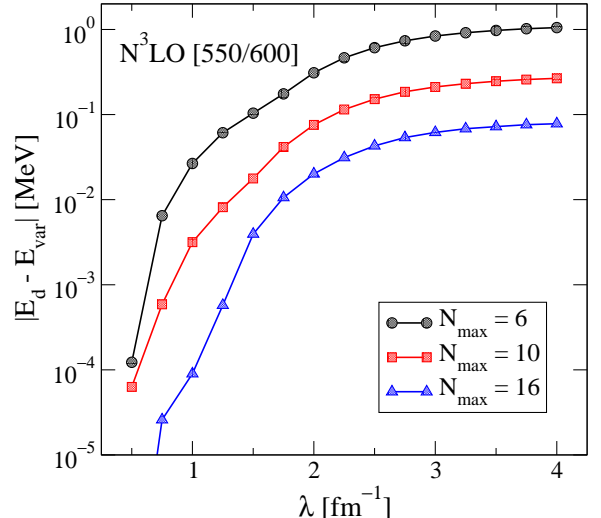


FIG. 5: The absolute error vs.  $\lambda$  of the predicted deuteron binding energy from a variational calculation in a fixed-size basis of harmonic oscillators ( $N_{\text{max}} \hbar \omega$  excitations). The initial potential is from Ref. [13].

The more perturbative potentials at lower  $\lambda$  induce weaker short-range correlations in few- and many-body wave functions, which in turn leads to greatly improved convergence in variational calculations. This is illus-

trated via calculations of the binding energy of the deuteron and triton by diagonalization in a harmonic oscillator basis, as shown in Figs. 5 and 6. For a fixed basis size, a more accurate estimate is obtained with smaller  $\lambda$  or, conversely, at fixed  $\lambda$  the convergence with basis size becomes more rapid. The improvement in convergence is similar to that found with smoothly regulated  $V_{\text{low } k}$  potentials [7]. At finite density, analogous effects led to perturbative behavior in nuclear matter for  $V_{\text{low } k}$  potentials [5]. Preliminary results support a similar conclusion for the SRG potentials [14].

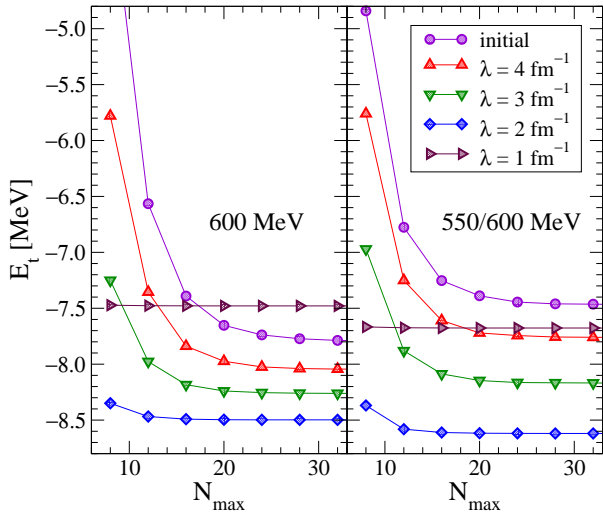


FIG. 6: The variational binding energy for selected  $\lambda$  of the triton with two-nucleon interactions only, as a function of the size of the harmonic oscillator space ( $N_{\text{max}}\hbar\omega$  excitations), for the same initial potentials as in Fig. 1.

In Fig. 6, the calculations for different  $\lambda$  converge to different values for the binding energy of the triton. This reflects the contributions of the omitted (and evolving) three-body interaction. The evolution with  $\lambda$  of the binding energy with NN interactions only, which is also the

evolution of the net three-body contribution, follows a similar pattern to that seen with  $V_{\text{low } k}$  [4, 7]: a slow decrease as  $\lambda$  decreases, reaching a minimum for  $\lambda$  between  $1.5 \text{ fm}^{-1}$  and  $2 \text{ fm}^{-1}$ , and then a rapid increase.

The consistent RG evolution of few-body interactions is an important unsolved problem for low-momentum potentials. In  $V_{\text{low } k}$  calculations to date, an approximate evolution is made by fitting the leading chiral EFT three-body force at each cutoff while evolving the two-body interaction exactly [4]. Generalizing the RG evolution to include the three-body interaction is, at least, technically challenging. However, in contrast to the machinery used to construct  $V_{\text{low } k}$ , the SRG method does not require the solution of the full three-nucleon problem (i.e., bound state wave functions plus all scattering wave functions in all breakup channels) to consistently evolve the three-nucleon interactions. Thus, the concomitant evolution of three-nucleon interactions becomes practical by applying Eq. (5) in the three-particle space.

In summary, the SRG applied to nucleon-nucleon potentials works as advertised even for a simple choice of transformation, driving the hamiltonian (in momentum space) towards the diagonal, making it more perturbative and more convergent in few-body calculations. There is much to explore, such as the nature of the decoupling of high- and low-energy physics implied by Fig. 1 and whether other choices of  $\eta$  in Eq. (4) could be more effective in making the hamiltonian diagonal. For example, the replacement  $T_{\text{rel}} \rightarrow H_d$ , where  $H_d$  is the diagonal part of the hamiltonian, or some function of  $T_{\text{rel}}$  [14] are easily implemented. Most important is the consistent evolution of non-hamiltonian and three-body operators.

## Acknowledgments

We thank A. Schwenk for useful comments. This work was supported in part by the National Science Foundation under Grant No. PHY-0354916.

---

[1] E. Epelbaum, W. Glöckle, A. Krüger and U.G. Meißner, Nucl. Phys. **A645**, 413 (1999).  
[2] S. K. Bogner, T. T. S. Kuo and A. Schwenk, Phys. Rept. **386**, 1 (2003).  
[3] S. K. Bogner, A. Schwenk, T. T. S. Kuo and G. E. Brown, nucl-th/0111042.  
[4] A. Nogga, S. K. Bogner and A. Schwenk, Phys. Rev. C **70**, 061002(R) (2004).  
[5] S. K. Bogner, A. Schwenk, R. J. Furnstahl and A. Nogga, Nucl. Phys. **A763**, 59 (2005).  
[6] S. K. Bogner, R. J. Furnstahl, S. Ramanan and A. Schwenk, Nucl. Phys. **A773**, 203 (2006).  
[7] S. K. Bogner, R. J. Furnstahl, S. Ramanan and A. Schwenk, arXiv:nucl-th/0609003.  
[8] S. D. Glazek and K. G. Wilson, Phys. Rev. D **48**, 5863 (1993); Phys. Rev. D **49**, 4214 (1994).  
[9] F. Wegner, Ann. Phys. (Leipzig) **3**, 77 (1994).  
[10] S. Szpigel and R. J. Perry, in *Quantum Field Theory, A 20th Century Profile* ed. A.N. Mitra, Hindustan Publishing Com., New Delhi, 2000), arXiv:hep-ph/0009071.  
[11] An alternative non-RG use of unitary transformations to reduce correlations in many-body wave functions is described in R. Roth, H. Hergert, P. Papakonstantinou, T. Neff and H. Feldmeier, Phys. Rev. C **72**, 034002 (2005), and references therein.  
[12] D. R. Entem and R. Machleidt, Phys. Rev. C **68**, 041001(R) (2003).  
[13] E. Epelbaum, W. Glöckle and U. G. Meißner, Nucl. Phys. **A747**, 362 (2005).  
[14] S. K. Bogner, R. J. Furnstahl, and R. J. Perry, in preparation.  
[15] S. Weinberg, Phys. Rev. **131**, 440 (1963).